Korean J. Chem. Eng., 35(4), 941-955 (2018)
DOI: 10.1007/s11814-017-0261-4

pISSN: 0256-1115
eISSN: 1975-7220

Techno-economic evaluation of gas separation processes for long-term operation of CO_2 injected enhanced coalbed methane (ECBM)

Sunghoon Kim*,‡, Daeho Ko,‡, Junyoung Mun*, Tae-hyun Kim***, and Jiyong Kim*,†**

*Department of Energy & Chemical Engineering, Incheon National University,
119, Academy-ro, Yeonsu-gu, Incheon 22012, Korea
**Global Engineering Division, GS Engineering & Construction, 33, Jong-ro, Jongno-gu, Seoul 03159, Korea
***Organic Material Synthesis Laboratory, Department of Chemistry, Incheon National University,
119, Academy-ro, Yeonsu-gu, Incheon 22012, Korea

(*Received 10 August 2017 • accepted 20 September 2017*)

Abstract−Energy source diversification through development of coalbed methane (CBM) resources is one of the key strategies to make a country less dependent on simple energy resources (e.g., crude oil, natural gas, nuclear energy etc.). Especially, enhanced coalbed methane (ECBM) technology can be expected to secure the resources as well as environmental benefits. However, the raw CBM gas obtained from CO_2 ECBM contains a considerable amount of CO_2, and the CO_2 content increases depending on the operation time of the facility. Considering the changes of the CBM composition, we developed process simulations of the CBM separation & purification processes based on the amine absorption to meet the design specifications (CH_4 purity of product stream: 99%, CH_4 recovery rate: 99%) with different CBM feed gas conditions. Using the developed simulation model, we performed an economic evaluation using unit methane production cost (MPC) considering coal-swelling types and facility operation time, and established an operation strategy under different natural gas market scenarios.

Keywords: Energy Diversification, Coal Bed Methane, Gas Separation, Energy System, Economic Evaluation

INTRODUCTION

With global population and consumption expected to significantly increase, the current energy system supported by the conventional energy resources could face critical energy-related crisis in the near future owing to the insufficiency of fossil fuel reservoirs [1,2]. Accordingly, the development of new energy resources that are not conventionally utilized is very important to maintain the operation of the current energy system in a sustainable manner by a continuous feed of necessary resources. Coalbed methane (CBM) is one of the promising alternative energy resources to replace or cooperate with the current gas industry and market [3]. The amount of methane (CH_4) produced from the CBM approximately accounts for 9% of the total natural gas production, and the CBM resources are estimated to exceed 9,000 trillion standard cubic feet (Tscf), i.e., approximately 36% of the total natural gas reserves available globally [4]. By contrast, owing to the regional imbalances of the natural gas reserves, the use of CBM resources is widely spread, and this aids in improving the energy security and flexibility [5-8].

Furthermore, the CBM recovery rate can significantly be improved owing to the injection of replacement gases (CO_2 and N_2) into the coal seams, which is called the enhanced coalbed methane (ECBM) technology [9,10]. For example, injecting CO_2 into the coal seams can increase the CH_4 recovery rate by 23-30% compared to the natural depletion [9,11]. The CO_2 ECBM has been considered as a green technology because the injected CO_2 could be sequestrated in the coal seam, which can reduce the greenhouse gas emissions [12]. Thus, the CO_2 ECBM can result not only in the improvement of the economics of CH_4 supply, but also contribute to the mitigation of climate change [13].

The CBM gas produced by the CO_2 ECBM contains a considerable amount of CO_2 [7]. Therefore, a gas processing plant for producing high-purity CH_4 gas from the raw CBM gas is essential to using the CBM gas as the CH_4 supply option. There have been numerous studies on topics related to the design and assessment of the CBM treatment processes. Congmin et al. (2012) conducted research to obtain separation efficiency between CH_4 and N_2 using pressure swing adsorption (PSA). They identified the relationship between the separation efficiency and the carbon pore structure experimentally and theoretically [14]. Ko (2016) developed a new mathematical model to calculate the design parameters (e.g. bed length, inside diameter) of PSA using gPROMS. This study can be used to scale up the vacuum pressure swing adsorption (VPSA) designed for the CBM separation [15]. Robertson (2007) analyzed the cost of separation and transportation of the CO_2 which is the ECBM injection gas. Especially, the study evaluated the economics of the flue gas separation and transportation via various separation technologies (PSA, membrane, aqueous amine, etc.) to deter-

†To whom correspondence should be addressed.
E-mail: jykim77@incheon.ac.kr
‡Authors contributed equally to the manuscript.

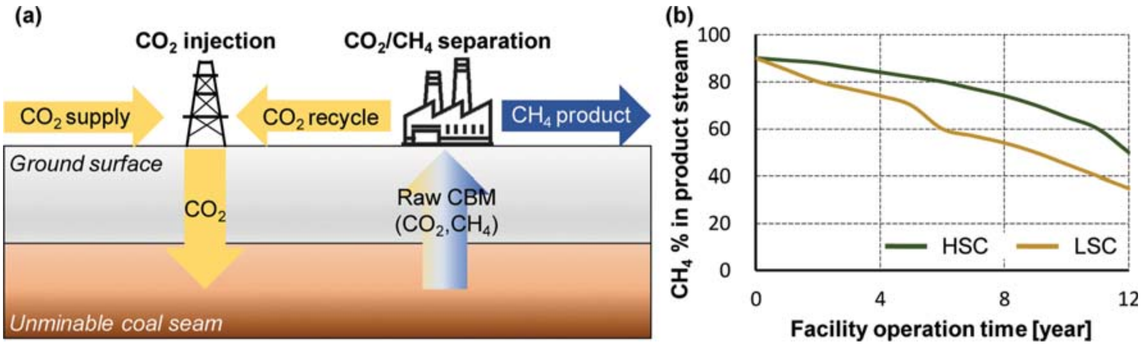

Fig. 1. (a) CO_2-injected ECBM process and (b) changes of methane in raw CBM gas in the long-term operation. HSC: High swelling coal seam; LSC: Low swelling coal seam [23,25].

mine the effect of the CO_2 injection [16]. Zhang et al. (2013) proposed an optimal design strategy for the CBM separation to obtain a superstructure model consisting of three separation technologies (PSA, membrane, cryogenic); this optimal design was obtained using mixed integer nonlinear programming (MINLP) method [17].

While a number of studies associated with the development of the CBM separation processes are found in the literature, there is still a lack of studies to provide the practical solutions to address the issues on the design and operation of the CO_2 ECBM. Wei et al. investigated the CH_4 recovery depending on the type and period of gas injected into the ECBM using a developed dynamic multicomponent transport (DMCT) model to understand the gas behavior and analyze the effect of factors (e.g. injection gas composition, pressure) [18]. Zhou et al. (2013) predicted the CBM production behavior for different injection gas composition and different injection starting time using laboratory data and dynamic model [19]. The economic feasibility is significantly affected by the variations in the CH_4 content in the feed. For example, as the feed CO_2 content increases from 5% to 50%, the production cost of CH_4 also increases from 0.15 USD/MMBTU (US dollars per million British thermal unit) to 1.44 USD/MMBTU [20].

Accordingly, it is important to establish appropriate long-term planning strategies considering temporal changes in the CO_2 concentration during the ECBM process. The operation strategy should be carefully investigated in the initial decision-making stage including the development of a process design model. Therefore, our objective was to provide strategically practical solutions for planning the CBM separation process with changes in the feed CO_2 content. To achieve this goal, we first developed aqueous amine solution-based process simulations of the CBM separation & purification and investigate the variations in the CO_2 content according to the operating time and coal conditions (Section 2). Secondly, we discussed the energy consumption and efficiency based on the results obtained from the process simulation (Section 3). We subsequently conducted an economic evaluation of certain scenarios by combining the project life period and coal conditions and identify the primary cost drivers based on the results of Section 3 (Section 4). Finally, we performed an extended economic evaluation to establish the optimal supply and selling strategies under different natural gas market scenarios (Section 5).

CO_2-INJECTED ECBM AND GAS SEPARATION SYSTEM

1. CBM Production Behavior in the ECBM Process

Fig. 1(a) shows the schematic diagram of a typical CO_2 ECBM process. Before the normal operation of the CO_2 ECBM process, a significant amount of water is discharged from within the coal seam. We assumed that the extracted CH_4 in the initial stage is not included, because the amount of CH_4 produced along with water is negligible in comparison to the total amount of CH_4 required for the long-term operation. After the dewatering process, the CH_4 is readily released from the adsorption sites in the coal seam owing to the decreased partial pressure of CH_4 due to the injected CO_2; two moles of the injected CO_2 replace one mole of the adsorbed CH_4 [22]. The displaced CH_4 is pumped out to multiple raw CBM production wells as a free gas phase, while the injected CO_2 is sequestered in the coal seams.

The extracted raw CBM stream, a mixture of CO_2 and CH_4, should be processed on-site for technical and economic purposes: high purity of CH_4 for pipelines transportation and large amount of the recycle CO_2 to minimize CO_2 purchasing. The CBM gas production in the CO_2-injected ECBM site is sensitive to the amount of the injected CO_2 and the conditions of coal seams such as coal swelling type, density, moisture content, and coal volumetric (thickness and areal extent) [21,22]. To correctly consider CH_4 behavior in the coal seam, we adopted the estimation method and assumptions used in previous researches [18,19]. Thus, we assumed two types of coal swelling (low and high swelling types), since the coal swelling type has significant effect on determining the speed at which the coal can absorb the CO_2 gas and the effects of desorption changes on the gas flow rates in the reservoir [23,24]. For example, the CO_2 adsorption and CH_4 desorption occurs more actively in the high swelling coals (HSC) than in the low swelling coals (LSC), which indicates that the CH_4 content of the CBM gas in the case of HSC is higher than that in the case of LSC. Fig. 1(b) shows the changes of the CH_4 content in the raw CBM gas during the long-term operation of the ECBM process. As the operation time of the facility increases, the proportion of the CH_4 in both swelling coal beds steadily decreases from 90% to 50% and 34%, respectively.

2. CO_2-CH_4 Separation System Overview

CO_2 absorption using amine solution is a rather mature tech-

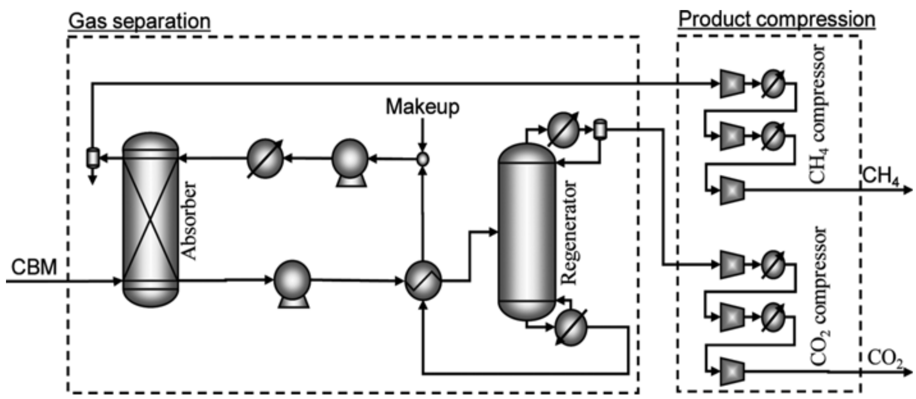

Fig. 2. Simplified process flow diagram of the amine-based CO_2-CH_4 separation system for CO_2 ECBM application.

nology for CO_2 separation, widely used in CO_2 capture from the flue gas of coal fired power plants. Fig. 2 shows the CO_2 and CH_4 separation system proposed in this study. The CBM gas is supplied into the bottom of the absorption column, and the CO_2 dissolves in the amine solution through chemical absorption reaction [26]. In the absorption column, uncaptured CO_2, steam, mono ethanol amine (MEA), and the selected amine for CO_2 absorption, are emitted from the top section and the amine solution including CO_2 is discharged from the bottom section. The CH_4 purity is improved by installing a tank to separate the treated gas at the top section. The treated gas is pressurized up to 1.7 MPa and subsequently transported through a pipeline to the demand areas. The amine solution absorbing the CO_2 coming from the bottom of the absorption column is pre-heated and subsequently enters the stripping column. In the stripping column, the CO_2 is discharged from the top section through reverse absorption reaction. The amine solution is regenerated in the stripping column, emitted from the stripping column bottom, cooled by heat exchanger, and subsequently transported into the absorption column with a make-up MEA and de-ionized water.

While the basic characteristics of the proposed CO_2-CH_4 separation system are similar to a typical amine-based CO_2 separation process, additional parts needs to be included for the CO_2 ECBM application;

- CH_4 compression: To directly connect to natural gas market, the pressure of separated CH_4 stream should be increased up to 1.7 MPa for meeting the pipeline specification [27]
- CO_2 compression: To recycle the separated CO_2 as an injection gas in the ECBM site, the pressure is increased up to 1.8 MPa [28].

PROCESS SIMULATION RESULTS

We conducted the modeling and simulation of the CO_2 and CH_4 separation system as shown in Fig. 2. In general, the amount of raw CBM gas from a unit well ranges from 106 to 600 Mcf/D; a CO_2 ECBM site includes numerous wells [29,30]. Thus, there is a wide range of variation in the amount of the CBM feed. To ensure practical results, for example, the economics of the commercial CO_2 ECBM process, this study assumes the CBM feed flow to be 12,100 Mcf/D (approximately 697 kmol/hr) [10]. For a product specification, the purity of the CH_4 in the production stream is set to

Table 1. Major mass flows in CO_2-CH_4 separation systems during long-term operation. HSC: High swelling coal seam; LSC: Low swelling coal seam

Year	HSC				LSC			
	CH_4 % in CBM feed	Recycled CO_2 (kton)	Produced CH_4 (kton)	Stream info.	CH_4 % in CBM feed	Recycled CO_2 (kton)	Produced CH_4 (kton)	Stream info.
1	90	24	79	Table S1	90	24	79	Table S1
2	88	29	78	Table S2	80	48	71	Table S6
3	86	34	76	Table S3	77	56	68	Table S7
4	84	39	74	Table S4	74	63	65	Table S8
5	82	44	72	Table S5	70	73	62	Table S9
6	80	48	71	Table S6	60	97	53	Table S11
7	77	56	68	Table S7	57	104	50	Table S12
8	74	63	65	Table S8	54	111	48	Table S13
9	70	73	62	Table S9	50	121	44	Table S14
10	65	85	57	Table S10	45	133	40	Table S15
11	60	97	53	Table S11	40	145	35	Table S16
12	50	121	44	Table S14	35	157	31	Table S17
Total		711	799			1,132	645	

99.9% to be directly used as an energy resource.

1. Mass Flows and Utility Consumption

Because the ratio of CO_2 and CH_4 of the raw CBM gas changes during the long-term operation of the ECBM process, we developed 17 process models according to the composition of the CBM feed gas from 90% to 35% CH_4 purity in the CBM feed stream; the process model along with the mass and energy information was developed using Aspen Plus V 8.0 [31]. While important results are discussed here, the detailed situation results of the 17 process models, including the process flow diagrams and information on the major streams, are provided in Fig. A1 and Tables A1-A17 in the online supplementary material.

As shown in Table 1, the annual production of the 99% purity CH_4 decreases as the operation years proceed; the produced amount in the previous year (44,000 ton/year) decreased by 55.7% compared with that of the first year. Further, the amount of the separated CO_2, which will be recycled in the CO_2 injection process, annually increases. While the LSC case shows similar production profile, the obtained CH_4 amount is comparatively lower than that in the HSC case due to its related low CH_4 % in the feed stream (See Fig. 1(b)).

The utility of the process models is that they consist primarily of electricity for pressure change, steam for heating, and cooling water. In particular, the electricity consumed for CH_4 and CO_2 pressure-up and the steam used in the reboiler of the regenerator (See Fig. 2) are substantially critical utilities against cooling water. Figs. 3(a) and 3(b) show the amount of electricity consumed in the compressors of both the LSC and HSC cases, respectively. As the operation time increases, the total amount of consumed electricity in both cases decreases; at the final year, it is reduced by 9.4% and 12% compared to the starting year, respectively. This is attributed to the decrease in the amount of CH_4 product flow despite the increase of the separated CO_2. The unit electricity consumption for purifying CH_4 is higher than that of the separated CO_2; note that the pressuring of 1 kg of CH_4 and CO_2 by 1 bar consumes 0.04 kW and 0.01 kW, respectively. The difference in the consumption profile between the HSC and LSC is observed in Figs. 3(a) and (b). In the HSC case, the electricity consumption for CH_4 compressing is dominant across all the examined years, whereas the dominant operation of the HSC case steadily changes from CH_4 compression to CO_2 compression.

Figs. 3(c) and (d) show the amount of steam used in the regenerator unit in the cases of HSC and LSC, respectively. As the operation of the gas separation system proceeds, the amount of the used steam gradually increases in both the cases, because of the increasing CO_2 content in the CBM feed. The steam is only dependent on the amount of the amine solution. Thus, the amount of steam used in the LSC case is higher than that of the HSC case owing to higher CO_2 ratio in the feed of the LSC case than the HSC case.

2. Energy Efficiency

As discussed, the amount of product and consumed utilities (electricity and steam) change during the system operation. For the concise comparison of technical performance between the two cases, we calculate the energy efficiency, using Eq. (1) [32].

$$\text{Process energy efficiency} = \frac{\text{Chemical energy of product}}{\text{Chemical energy of feed + Energy consumed in process}} [\%] \tag{1}$$

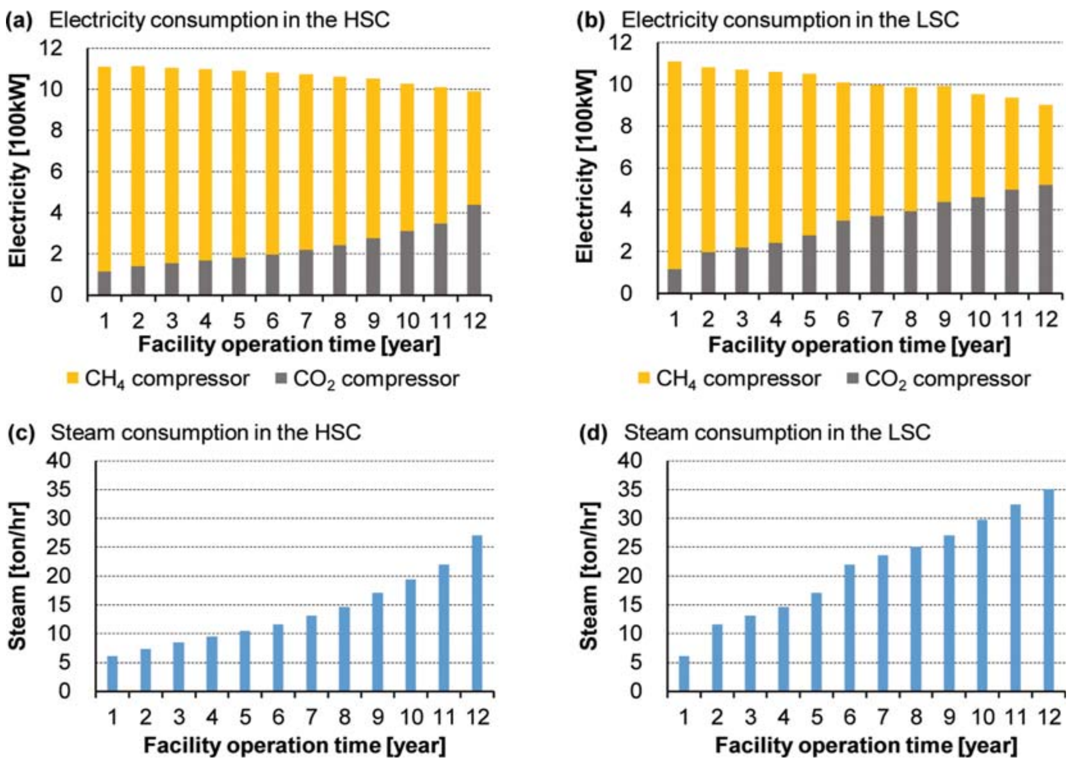

Fig. 3. Utility consumption of CBM separation system during facility operation time.

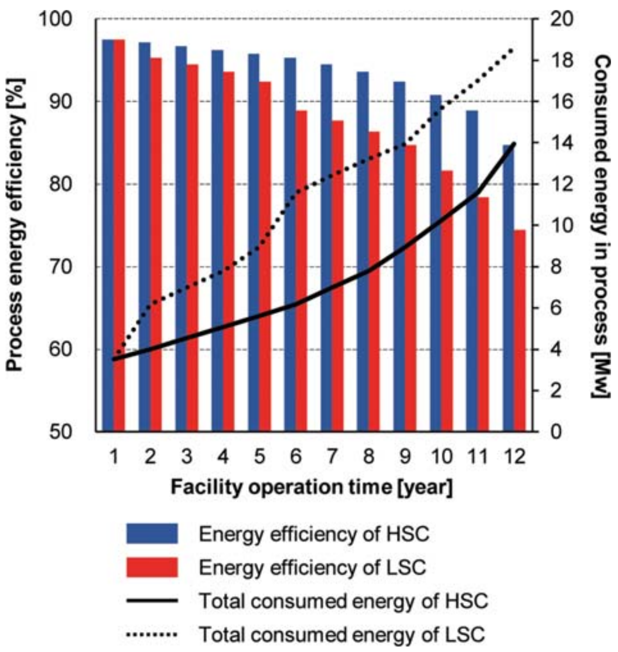

Fig. 4. Change of the energy efficiency in HSC and LSC cases.

where *chemical energy of product* and *chemical energy of feed* is the separated CH_4 and the raw CBM feed, respectively, and *energy consumed in process* includes all the utilities regarding the equipment of the gas separation system such as compressor, pump of electricity use, and reboiler attached regenerator and heater of stream use. Here, we assumed that the high heating value (HHV) of CH_4 and CO_2 is 55.5 and 0 MJ/Kmol, respectively.

Fig. 4 and Tables A18-A19 show the changes in the process energy efficiency during the process system operation. The high energy efficiency of the initial year (98%) gradually decreases till the last operation year in both the cases owing to the decrease of the product amount and the increase of total consumed energy. Note that the total energy consumed in the system operation is gradually increased, primarily due to a considerable amount of steam despite the decreasing electricity consumption (See Fig. 3). Therefore, it is evident that although two pressure-up processes (CO_2 and CH_4 compressing) are included in the gas separation system, steam is still a critical utility to determine the system energy efficiency. In the final year (12th year), the energy efficiency in the HSC and LSC cases decrease by 13% and 24% compared to the starting year, respectively. In particular, the energy efficiency of the LSC case shows a considerable decrease compared to that in the HSC case owing to the large increment of utility consumption.

ECONOMIC EVALUATION

1. Parameters and Assumptions

For the economic evaluation, we considered three types of costs with regard to the construction and operation of the CBM gas separation process: total capital investment cost (TCI), operating cost, and raw material cost, which are calculated based on equipment and flows data obtained from the developed process model.

The total capital investment cost consists of i) direct costs (e.g., purchased equipment, installation cost, instrument and control, piping installed, electrical installation, building and building services, yard improvements, services facilities and land cost), ii) indirect costs (engineering, construction expenses, contractor's fee and contingency), and iii) working capital. The operating cost is classified into three contributors: i) fixed operating cost (labor, operating charge, and general & administration) and ii) variable operating cost (MEA make-up, de-ionized water costs, electricity, steam and cooling water), and auxiliary costs (plant overhead and maintenance cost). The raw material cost is calculated by the amount of the raw CBM feed and the unit required cost to supply the raw gas to the gas separation system. The total capital investment cost is calculated based on the values in Table 2.

The major assumptions and values for the economic evaluation are summarized in Table 3.

Table 4 shows the major material and utility costs in this study. The raw CBM supply cost includes the pretreatment process of the

Table 2. Factors to calculate total capital investment cost [33,34]

	Percentage [%]
Direct cost [% of PE]	268.8
Purchased equipment (PE)	100
Equipment installation [% of PE]	52.8
Instrumentation and control [% of PE]	20
Piping [% of PE]	40
Electrical installation [% of PE]	11
Building and building services [% of PE]	10
Yard improvements [% of PE]	10
Services facilities [% of PE]	20
Land [% of PE]	5
Indirect cost [% of PE]	100.8
Engineering [% of PE]	26.88
Construction expenses [% of PE]	26.88
Contractor's fee [% of PE]	1.34
Contingency [% of PE]	45.7
Fixed capital investment cost (FCI) =Direct cost+Indirect cost [% of PE]	369.6
Working capital [% of PE]	92.4
Total capital investment cost (TCI) =Fixed capital investment cost+Working capital	462

Table 3. Assumptions and parameters for economic evaluation [35]

Parameters	Value
Project's economic life [year]	20
Operating charges [% of operating labor cost]	15
Plant overhead [% of labor and maintenance costs]	25
Tax rate [%/year]	25
Interest rate [%]	8
Operability [%]	90
Salvage value [% of TCI]	10
Depreciation	Straight line

Table 4. Raw material and absorbent price of the technologies [37, 38]

Parameters	Value
Raw CBM supply cost [USD/MMBTU]	0.5
MEA price [USD/kg]	0.97
De-ionized water price [USD/ton]	1
Electricity price [USD/kWh]	
Steam price [USD/ton]	
Cooling water price [USD/ton]	0.03

CBM gas (dewatering and washing) as well as the CBM extraction. An annual 2% escalation of the prices was assumed in this study, because we analyzed the economics of the gas separation system with respect to a long-term operation [36].

2. Economic Evaluation Results

As one of the major evaluation metrics, we estimated the methane production cost (MPC) [USD/MMBTU (US dollars per million British thermal unit)], which was calculated by dividing the total production cost by the amount of the produced CH_4. Total production cost includes net total capital investment cost, operating cost, and raw material costs. We estimated the equipment and operating expenses using Aspen Economic Evaluation V8.0.

Here, the project life period means the duration of the project from the initial investment year to the end year. We consider the salvage value that is calculated via the linear depreciation method if the end point of the project is shorter than the project's proposed life time (20 years), as assumed in section 4.1. To comparatively analyze the favorable project life time, i.e., favorable project termination year to ensure significant economy, we set four different project periods with regard to the CBM gas separation process: project period #1, #2, #3, and #4 of three-years, six-years, nine-years and twelve-years operation period, respectively. The numerical results of the economic evaluation of the four project lifetimes of the two swelling cases are summarized in Table A20.

Fig. 5 shows the MPC and the cost contribution in accordance with the different project periods. The calculated MPC demonstrates a wide range between 1.7 and 2.8 USD/MMBTU. In the HSC case with project period #1 (project is terminated after three years of operation), the project shows the lowest MPC owing to the raw CBM feed of the high-purity CH_4 and the substantially large salvage value. As shown in Fig. 5, the MPC in the LSC case is higher than that of the HSC case regardless of the length of the project period owing to the large utility consumption rate and thereby, a high operating cost. Moreover, the amount of the produced CH_4 in the LSC case is lower than that of the HSC case. The MPC in both the HSC and LSC cases becomes comparatively high, as a comparatively long project period is applied. Especially, the MPC in the LSC case rapidly increases compared to that in the case of the HSC, since the LSC case is more sensitive to the increase of the operating cost than the HSC case owing to the relatively small amount of the CH_4 product resulting from low CH_4 ratio in the raw CBM feed.

Fig. 5 also shows the main cost-drivers of the gas separation systems. In both the HSC and LSC cases, the VOC and RMC are the main contributors to MPC across all the examined project periods. Therefore, it is evident that the cost saving with regard to the raw CBM gas extraction and supply, and the utility is a critical factor for the improvement of the economics of the gas separation system, furthermore to ensure the cost-competitiveness of the CBM-derived CH_4 in a gas market.

EXTENDED ANALYSIS OF CBM-DERIVED CH_4 IN NATURAL GAS MARKET

Based on the cost information discussed in the previous section, in this section, we evaluate the feasibility of the market competitiveness of the CBM-derived CH_4 using various evaluation criteria, such as cash flow analysis, payback period, and net present value (NPV) analysis [39]. The market price of natural gas is an important factor to evaluate the competitiveness of the CH_4 produced in the CO_2 ECBM. According to the U.S. Energy Information Administration (EIA) report, 41% of the natural gas is produced by the United States, 32% by Russia, and less than 10% by other countries [40]. Under the circumstance, we consider two different natural gas markets, and accordingly, two different prices.

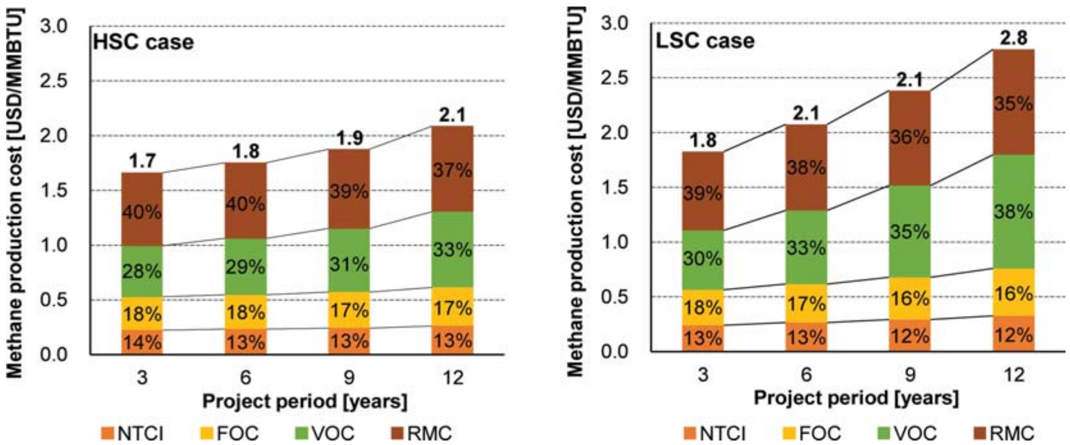

Fig. 5. Cost contribution to MPC with different project periods. NTCI: net total capital investment cost; FOC: fixed operating cost; VOC: variable operating cost; RMC; raw material cost.

Table 5. Scenarios for the economic evaluation

Sc.	Coal swelling case	NG market
HU	High	U.S.
HR	High	Russia
LU	Low	U.S.
LR	Low	Russia

The natural gas price in the U.S. and Russian markets, as investigated on June 2016, was 2.94 USD/MMBTU and 4.04 USD/MMBTU, respectively [45]. In this chapter, we develop an operational strategy with regard to the representative markets (i.e. the U.S. and Russia). By combining the two coal swelling types and the two markets, this study generates four scenarios as shown in Table 5.

1. Annual Cash Flow Analysis

The annual cash flow analysis compares the revenue and expenditure in the examined project period and is useful to comparatively analyze the capability of the projects to repay the TCI and confirm the stability with regard to the scale of cash flow [41]. Fig. 6 shows the annual cash flow based on two coal swelling cases (HSC and LSC) and in two markets (U.S. and Russia). First, it is observed that the revenue in the Russian market is larger than that of the U.S. market. Therefore, selling the product in the Russian market has a satisfactory profitability compared with the same in the U.S. market.

Across all the scenarios, the steady decrease of the revenue from the starting year to the final year is observed; for example, the revenue decreases from 12.2 to 6.8 million US dollars in the HU scenario, and from 16.8 to 6.5 MUSD in the LR scenario. The decrease of the revenue along with the gradually increasing expenditure makes the cash flow have a negative value after a ten-year operation period. Therefore, it is evident that the examined CO_2 ECBM project required to supply the CH_4 to a natural gas market should terminate its operation before a negative cash flow appears, to maintain a profitable project management.

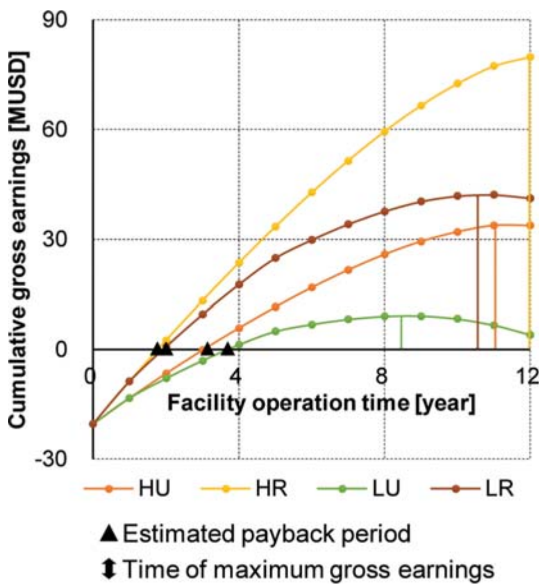

Fig. 7. Cumulative gross earnings and payback periods according to project operation period of four scenarios.

2. Payback Period Analysis and Gross Earnings

The optimal time to terminate the project is clearly verified using the payback period and the gross earnings analysis [42]. The pay-

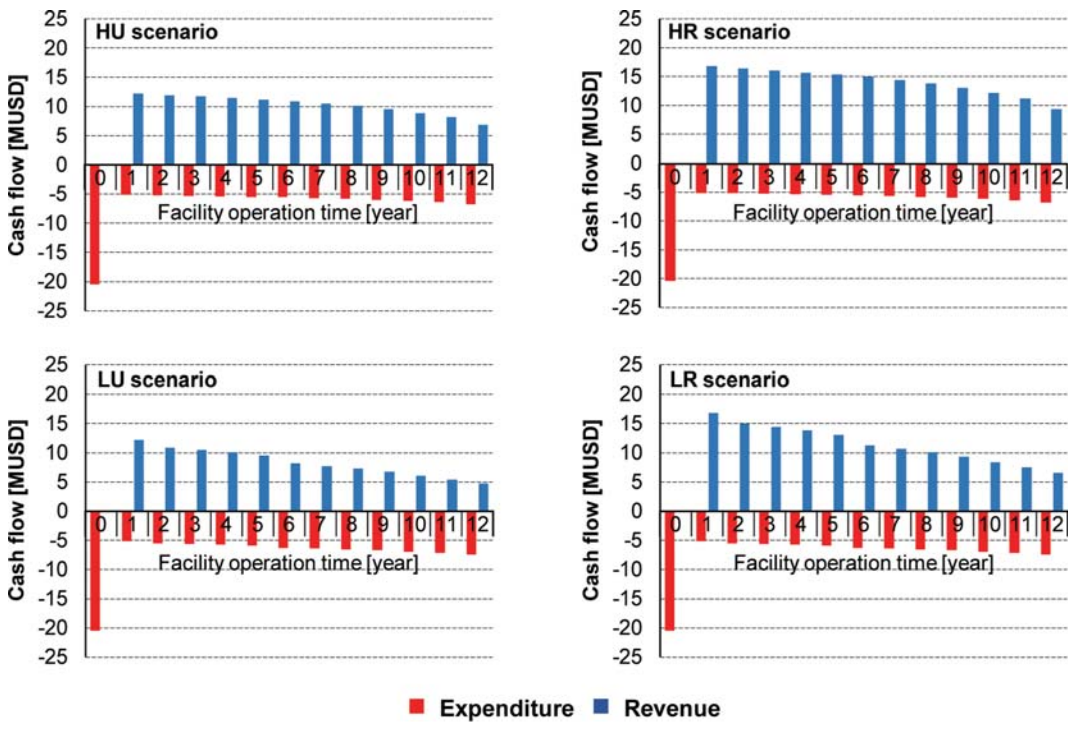

Fig. 6. Annual cash flow during facility operation time for different scenarios.

back period method indicates the time it will take to earn back the TCI of the project. The shorter the payback period, the more the investment value of the project will be rated as positive. Note that the payback period method only considers cash flows (revenue, expenditure), and does not consider the effect of depreciation of cash. However, it is advantageous in that it can easily identify the onset of the revenue [47].

Fig. 7 shows the payback period and the maximum gross earnings of the four scenarios. The payback period in the HR scenario is estimated to be 1.8 years, which is the shortest, followed by the LR of 1.9 years. Selling the product in the Russian market (average 1.9 years) has the shorter payback period than that of the U.S. market (average 3.4 years).

From Fig. 7, the termination timing to ensure the maximum gross earnings is different in accordance with the scenario; the maximum gross earnings in the HU, HR, LU, and LR scenarios are 11, 12, 9, and 11 years, respectively. The HR scenario shows the largest gross earnings with the longest project operation time (80.0 MUSD in twelve-year operation), whereas the LU scenario has the lowest maximum gross earning (9.1 MUSD) with the shortest project operation. Fig. 7 also shows the changes in the maximum gross earning with regard to different markets. The earning in the U.S. market is expected to be lower than that in the Russian market owing to the low selling price in the U.S. market.

3. Net Present Value Analysis

In the previous sections, it was analyzed that that the econom-

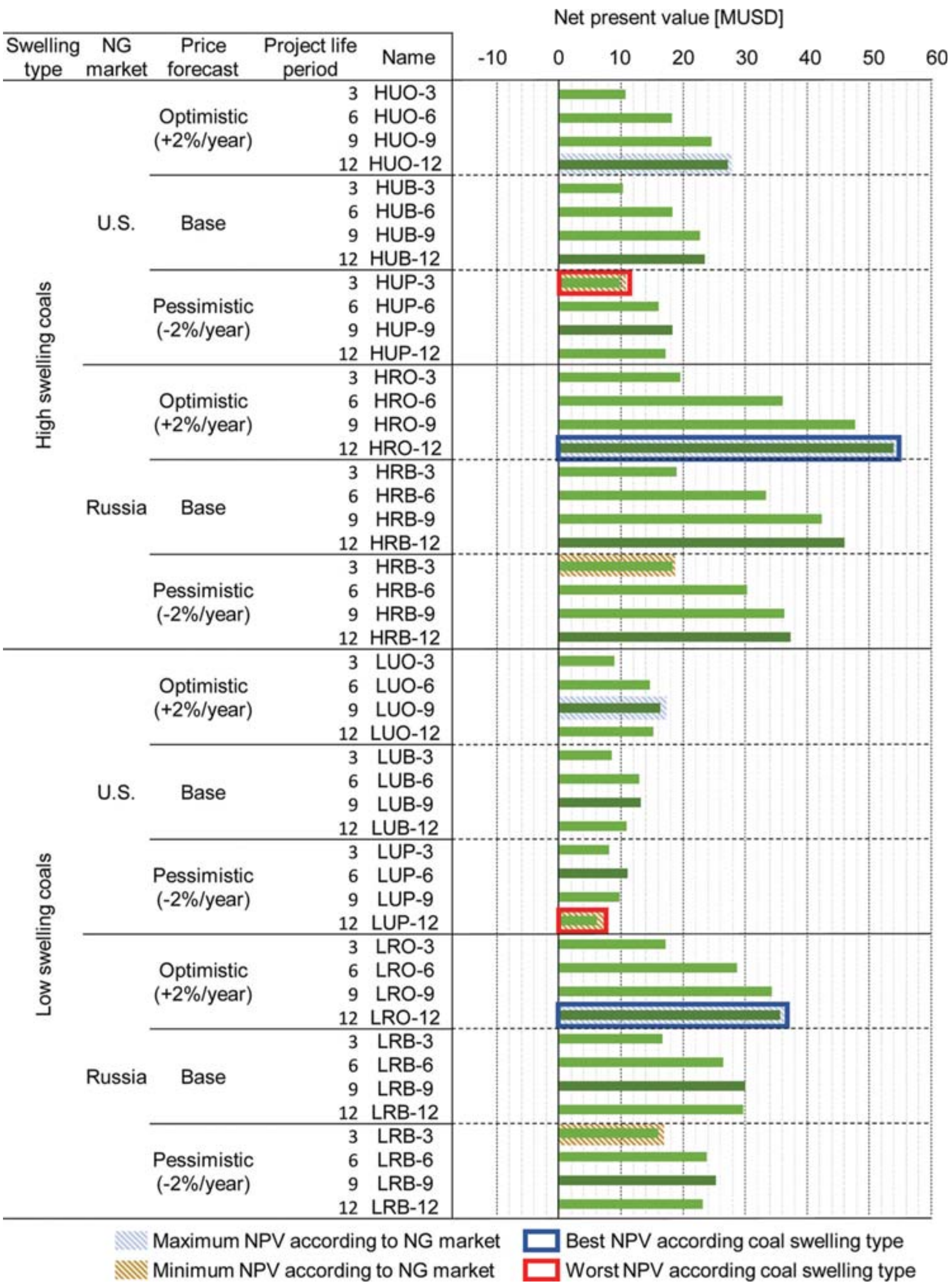

Fig. 8. Net present value of the proposed 48 projects of CH_4 production process.

ics of the CH_4 produced from the CO_2 ECBM project is exceedingly sensitive to the coal swelling types and the natural gas market prices. To establish the practical planning of the CH_4 production from the CO_2 ECBM project, it is necessary to consider the extended market scenarios such as the natural gas price change. Note that the selling price of natural gas in reality is exceedingly volatile with regard to the trade markets [43]. Thus, we extensively generated 48 scenarios by combining the two coal swelling cases (HSC and LSC), two natural gas markets (U.S. and Russia), and three price forecasts of natural gas (optimistic, base, and pessimistic), along with four project life periods (three, six, nine, and twelve years). We subsequently compared the NPV of the project of the CBM-derived CH_4 production using NPV analysis. The NPV method, which is a financial method that arranges a series of incoming and outgoing cash flows, is defined as the sum of the net benefit of the individual cash flows reflecting depreciation [44,45]. Investment with a positive NPV will be a lucrative project, and investment with a negative NPV will cause a deficit.

Fig. 8 shows the NPV of the CH_4 production project with regard to the 48 scenarios. The calculated NPV ranges widely from 6.1 to 54.0 MUSD. First, all the scenarios have a positive NPV. Thus, the CH_4 production in the CBM gas is a lucrative project for all the examined conditions. In general, the high coal swelling scenario demonstrates a better NPV value than the low scenario. For instance, HUO-3 and LUO-3, under the same market (U.S.), same price forecast (optimistic), and same project period (three-year), has NPV of 10.7 and 8.9 MUSD, respectively. The reason is that the gas separation process in the HSC case is more economic than that in the LSC case, as discussed in the previous sections. Comparing the U.S. and Russian markets, the projects in the Russian market have an NPV greater than that of the U.S. market by 43% from 73% for instance, HRO-3 shows NPV of 19.6 MUSD that is 45% greater than that of the HUO-3. Furthermore, in the LSC case the projects in the Russian market have a high NPV up to 73% compared with the U.S. market. Second, the effect of the changes in the natural gas price is also observed. For instance, HUP-3, HUB-3, and HUO-3 have different NPV values of 10.7, 10.3, and 9.8 MUSD, respectively. Especially, the effects become evident when the scenarios of the relatively long project periods are compared. For instance, there is a difference of up to 148% between LUO-12 (15.2 MUSD) and LUP-12 (6.1 MUSD). Therefore, when the market price of natural gas is forecasted to increase, the long-operation project could lead to improved economics.

Finally, we investigated the effects of the project period. In Fig. 8, the scenario colored dark green denotes the project that has the maximum NPV value among the four different project periods. When the natural gas price is expected to be optimistic, the projects of the longest operation period show the most significant NPV value against other projects of short-operation strategies. Further, in the pessimistic scenarios, the maximum NPV appears in the projects with relatively short operation time. For example, in the HSC case and the U.S. market, the project life periods that have the maximum NPV (colored dark green) change from the longest scenario (HUO-12) to HUP-9 by assuming the bad market conditions of the natural gas price.

CONCLUSIONS

CBM gas is one of the promising alternatives to conventional natural gas. To establish an investment and operation strategy of the CO_2 ECBM project, we analyzed the feasibility of CBM-derived CH_4 in the natural gas market. We first developed a process model for the CO_2-CH_4 separation system to produce a high-purity CH_4 from the raw CBM gas. We subsequently evaluated the CBM gas separation system with various metric and criteria (MPC, accumulated cash flow, payback period, NPV) under numerous scenarios (different coal swelling cases, natural gas markets, and price forecasts, and project periods).

As a result, we determined that both the HSC and LSC cases show the highest energy efficiency (approximately 98%) in the initial operation period. However, the energy efficiency is gradually decreased to 85% and 74%, respectively, after a twelve-year operation owing to the decreasing CH_4 amount in the raw CBM feed. When the project period of the CBM-derived CH_4 production is assumed to be three, the HSC case shows the lowest MPC ($1.7/MMBTU) due to the operation using only the raw CBM feed with high-ratio CH_4 and the relative salvage value. Based on an extended analysis with regard to various scenarios, we also analyzed the sensitivity of the technical and market conditions towards NPV of the CBM-derived CH_4 production project, including coal swelling type, selling market, project period and price changes. As a result, the most promising and pessimistic scenarios were identified: HRO-12 with the highest NPV (38.7 MUSD) and LUP-12 with the lowest NPV (6.1 MUSD), respectively.

This study provides a preliminary approach to analyze the feasibility of the CBM-derived CH_4 as an alternative to existing natural gas using different techniques in process systems engineering, process modeling and simulation, energy efficiency analysis, economic evaluation methods (e.g., MPC, cash flow, payback period, and NPV). The proposed approach, along with the obtained results, can be used as a guideline for a pre-feasibility study in the initial decision-making stage to launch a CO_2 ECBM project, furthermore directly applied to the design and operation of the practical projects. Based on this study, future research might focus on the development of a rigorous process model for an entire CO_2 ECBM system from CO_2 supply and injection to the CBM extraction and water treatment, and applying different separation technologies such as pressure swing adsorption (PSA), membrane and cryogenics.

ACKNOWLEDGEMENT

The authors acknowledge the financial support of Converging Research Program (CRP-20141309) through Incheon National University of Korea.

REFERENCES

1. S. Mohr and G. Evans, *Energy Policy*, **38**(1), 265 (2010).
2. A. Midilli, M. Ay, I. Dincer and M. Rosen, *Renewable Sustainable Energy Rev.*, **9**(3), 255 (2005).
3. B. Liang, W. Sun, Q. Qi and H. Li, *Int. J. Min. Sci. Technol.*, **22**(6), 891 (2012).

4. C. Jenkins, C. Boyer, *J. Pet. Technol.*, **60**(2), 92 (2008).
5. K. Aminian and S. Ameri, *J. Nat. Gas Sci. Eng.*, **1**(1-2), 25 (2009).
6. D. Luo and Y. Dai, *Energy Policy*, **37**(10), 3883 (2009).
7. K. Kim, W. Sung and J. Han, *J. Korean Inst. Gas*, **17**(2), 36 (2013).
8. A. Al-Jubori, S. Johnston, C Boyer, S. Lambert, O. Bustos and J. Pashin, *Oilfield Rev.*, **21**, 4 (2009).
9. C. Sinayuc, J. Shi, C. Imrie, SA. Syed, A. Korre and S. Durucan, *Energy Procedia*, **4**, 2150 (2011).
10. M. Sayyafzadeh, A. Keshavarz, A. Alias, K. Dong and M. Manser, *J. Nat. Gas Sci. Eng.*, **27**(2), 1205 (2015).
11. P. Fulton, C. Parente, B. Rogers, N. Shah and A. Reznik, *A laboratory investigation of enhanced recovery of methane from coal by carbon dioxide injection* (1980).
12. A. Ranathunga, M. Perera, P. Ranjith and C. Wei, *Fuel*, **189**, 391 (2017).
13. U. Zahid, Y. Lim, J. Jung and C. Han, *Korean J. Chem. Eng.*, **28**(3), 674 (2011).
14. C. Liu, Y. Dang, Y. Zhou, J. Liu, Y. Sun and W. Su, *Adsorpt.*, **18**(3-4), 321 (2012).
15. D. Ko, *Ind. Eng. Chem. Res.*, **55**(4), 1013 (2016).
16. E. Robertson, *Idaho National Laboratory*, INL/EXT-08-13816, (2007).
17. G. Zhang, S. Fan, B. Hua, Y. Wang, T. Huang and Y. Xie, *J. Energy Chem.*, **22**(3), 533 (2013).
18. X. Wei, P. Massarotto, G. Wang, V. Rudolph and S. Golding, *Fuel*, **89**(5), 1110 (2010).
19. F. Zhou, W. Hou, G. Allinson, J. Wu, J. Wang and Y. Cinar, *Int. J. Greenhouse Gas Control*, **19**, 26 (2013).
20. E. First, M. Hasan and C. Floudas, *AIChE J.*, **60**(5), 1767 (2014).
21. S. Day, R. Fry and R. Sakurovs, *Int. J. Coal Geol.*, **74**(1), 41 (2008).
22. Z. Chen, Z. Pan, J. Liu, L. Connell and D. Elsworth, *Int. J. Greenhouse Gas Control*, **5**(5), 1284 (2011).
23. J. Xie, M. Gao, B. Yu, R. Zhang and W. Jin, *Geomech. Geophys. Geoenergy and Geo-resour.*, **1**(1-2), 15 (2015).
24. C. Karacan, *Int. J. Coal Geol.*, **72**(3-4), 209 (2007).
25. S. Karacan and F. Karacan, *Sci. Technol. Online*, **2**(2), (2012).
26. S. Park, H. Song, M. Lee and J. Park, *Korean J. Chem. Eng.*, **31**(1), 125 (2014).
27. T. He and Y. Ju, *Appl. Energy*, **115**, 17 (2014).
28. W. Nie, S. J. Peng, J. Xu, L. R. Liu, G. Wang and J. B. Geng, *Sci. World J.*, **2014**(1), Article ID 185608 (2014).
29. F. Mu, W. Zhong, X. Zhao, C. Che, Y. Chen and J. Zhu, *Nat. Gas Ind. B*, **2**(4), 383 (2015).
30. DOE U, Powder River Basin Coalbed Methane Development and Produced Water Management Study. US Department of Energy (2002).
31. Guide APU, *Aspen Technology. Inc.* (2009).
32. S. Kim, D. Ko, S. Row and J. Kim, *Chem. Eng. Res. Design*, **115**(A), 230 (2016).
33. P. Mores, N. Rodríguez, N. Scenna and S. Mussati, *Int. J. Greenhouse Gas Control*, **10**, 148 (2012).
34. H. Hwang, J. Han and I. Lee, I*nd. Eng. Chem. Res.*, **52**(51), 18334 (2013).
35. J. Kim, J. Miller, C. Maravelias and E. Stechel, *Appl. Energy*, **111**, 1089 (2013).
36. J. De Graaff, V. Zuazo, N. Jones and L. Fleskens, *J. Environ. Manage.*, **89**(2), 129 (2008).
37. D. Singh, E. Croiset, P. Douglas and M. Douglas, *Energy Convers. Manage.*, **44**(19), 3073 (2003).
38. S. Wong, D. Macdonald, S. Andrei, W. Gunter, X. Deng and D. Law, *Int. J. Coal Geol.*, **81**(3-4), 280 (2010).
39. R. Weijermars, *Appl. Energy*, **106**, 100 (2013).
40. US Energy Information Administration. Natural gas monthly 2016. http://www.eia.gov/ 2016 (2016).
41. N. Haeffelé, The Feasibility and the Economic Viability of Shipping LNG via the Northern Sea Route 2013.
42. R. Egging, F. Holz and S. Gabriel, *Energy*, **35**(10), 4016 (2010).
43. J. Kim, C. Henao, T. Johnson, D. Dedrick, J. Miller and E. Stechel and C. Maravelias, *Energy Environ. Sci.*, **4**, 3122 (2011).
44. S. Fleten and E. Näsäkkälä, *Energy Econ.*, **32**(4), 805 (2010).
45. H. Naims, *Environ. Sci. Pollut. Res.*, **23**(22), 22226 (2016).

APPENDIX A. TECHNICAL AND ECONOMIC RESULT OF PROCESS SIMULATION AND ECONOMIC EVALUATION

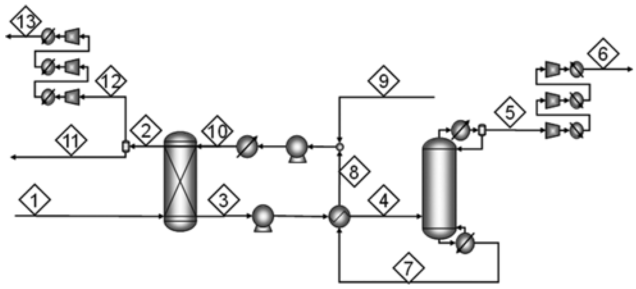

Fig. A1. Aspen flowsheet model of CBM gas separation process.

Table A1. Major stream information of CBM separation process (mole % of CH_4 in feed 90%)

Stream No.	1	2	3	4	5	6	7	8	9	10	11	12	13
Total flow (kmol/h)	697	657	1,740	1,740	72	70	1,668	1,668	32	1,700	24	633	629
Temperature (°C)	25	36	37	70	40	25	99	80	25	25	25	25	25
Pressure (kPa)	121	120	121	205	200	1,800	200	200	101	120	300	300	1,700
Component (kmol/h)													
CO_2	70	-	98	98	70	70	28	28	-	28	-	-	-
CH_4	627	627	-	-	-	-	-	-	-	-	-	627	627
H_2O	-	29	1,455	1,455	3	-	1,452	1,452	32	1,484	24	6	1
MEA	-	-	188	188	-	-	188	188	-	188	-	-	-

Table A2. Major stream information of CBM separation process (mole % of CH_4 in feed 88%)

Stream No.	1	2	3	4	5	6	7	8	9	10	11	12	13
Total flow (kmol/h)	697	642	2,088	2,008	87	84	1,921	1,921	32	1,953	24	618	613
Temperature (°C)	25	37	37	70	40	25	99	80	25	25	25	25	25
Pressure (kPa)	121	120	121	205	200	1,800	200	200	101	120	300	300	1,700
Component (kmol/h)													
CO_2	84	-	115	115	84	84	32	32	-	32	-	-	-
CH_4	613	613	-	-	-	-	-	-	-	-	-	613	613
H_2O	-	29	1,675	1,675	3	-	1,671	1,671	32	1,703	24	5	0
MEA	-	-	218	218	-	-	218	218	-	218	-	-	-

Table A3. Major stream information of CBM separation process (mole % of CH_4 in feed 86%)

Stream No.	1	2	3	4	5	6	7	8	9	10	11	12	13
Total flow (kmol/h)	697	628	2,295	2,295	101	98	2,194	2,194	32	1,700	23	604	599
Temperature (°C)	25	38	37	70	40	25	99	80	25	25	25	25	25
Pressure (kPa)	121	120	121	205	200	1,800	200	200	101	120	300	300	1,700
Component (kmol/h)													
CO_2	98	-	134	134	98	98	36	36	-	36	-	-	-
CH_4	599	599	-	-	-	-	-	-	-	-	-	599	599
H_2O	-	28	1,914	1,914	4	-	1,910	1,910	32	1,942	23	5	-
MEA	-	-	248	248	-	-	248	248	-	248	-	-	-

Table A4. Major stream information of CBM separation process (mole % of CH_4 in feed 84%)

Stream No.	1	2	3	4	5	6	7	8	9	10	11	12	13
Total flow (kmol/h)	697	613	2,583	2,583	116	112	2,467	2,467	32	2,499	23	590	586
Temperature (°C)	25	38	38	70	40	25	99	80	25	25	25	25	25
Pressure (kPa)	121	120	121	205	200	1,800	200	200	101	120	300	300	1,700
Component (kmol/h)													
CO_2	112	-	152	152	112	112	41	41	-	41	-	-	-
CH_4	585	585	-	-	-	-	-	-	-	-	-	585	585
H_2O	-	28	2,153	2,153	4	-	2,149	2,149	32	2,181	23	5	1
MEA	-	-	278	278	-	-	278	278	-	278	-	-	-

Table A5. Major stream information of CBM separation process (mole % of CH_4 in feed 82%)

Stream No.	1	2	3	4	5	6	7	8	9	10	11	12	13
Total flow (kmol/h)	697	599	2,871	2,871	130	125	2,741	2,741	32	2,773	22	577	573
Temperature (°C)	25	38	38	70	40	25	99	80	25	25	25	25	25
Pressure (kPa)	121	120	121	205	200	1,800	200	200	101	120	300	300	1,700
Component (kmol/h)													
CO_2	125	-	171	171	125	125	45	45	-	45	-	-	-
CH_4	572	572	-	-	-	-	-	-	-	-	-	572	572
H_2O	-	27	2,392	2,392	5	-	2,388	2,388	32	2,420	22	5	1
MEA	-	-	308	308	-	-	308	308	-	308	-	-	-

Table A6. Major stream information of CBM separation process (mole % of CH_4 in feed 80%)

Stream No.	1	2	3	4	5	6	7	8	9	10	11	12	13
Total flow (kmol/h)	697	585	3,137	3,137	144	139	2,993	2,993	32	3,025	22	563	559
Temperature (°C)	25	38	38	70	40	25	99	80	25	25	25	25	25
Pressure (kPa)	121	120	121	205	200	1,800	200	200	101	120	300	300	1,700
Component (kmol/h)													
CO_2	139	-	188	188	139	139	49	49	-	49	-	-	-
CH_4	558	558	-	-	-	-	-	-	-	-	-	558	558
H_2O	-	27	2,610	2,610	5	-	2,605	2,605	32	2,637	22	5	1
MEA	-	-	339	339	-	-	339	339	-	339	-	-	-

Table A7. Major stream information of CBM separation process (mole % of CH_4 in feed 77%)

Stream No.	1	2	3	4	5	6	7	8	9	10	11	12	13
Total flow (kmol/h)	697	563	3,590	3,590	166	160	3,424	3,424	32	3,456	22	541	537
Temperature (°C)	25	39	39	70	40	25	99	80	25	25	25	25	25
Pressure (kPa)	121	120	121	205	200	1,800	200	200	101	120	300	300	1,700
Component (kmol/h)													
CO_2	160	-	217	217	160	160	56	56	-	56	-	-	-
CH_4	537	537	-	-	-	-	-	-	-	-	-	537	537
H_2O	-	26	2,990	2,990	6	-	2,984	2,984	32	3,016	22	4	0
MEA	-	-	383	383	-	-	383	383	-	383	-	-	-

Table A8. Major stream information of CBM separation process (mole % of CH_4 in feed 74%)

Stream No.	1	2	3	4	5	6	7	8	9	10	11	12	13
Total flow (kmol/h)	697	541	4,022	4,022	188	181	3,834	3,834	32	3,866	21	520	517
Temperature (°C)	25	40	39	70	40	25	99	80	25	25	25	25	25
Pressure (kPa)	121	120	121	205	200	1,800	200	200	101	120	300	300	1,700
Component (kmol/h)													
CO_2	181	-	244	244	181	181	63	63	-	63	-	-	-
CH_4	516	516	-	-	-	-	-	-	-	-	-	516	516
H_2O	-	25	3,349	3,349	7	-	3,343	3,343	32	3,375	21	4	1
MEA	-	-	428	428	-	-	428	428	-	728	-	-	-

Table A9. Major stream information of CBM separation process (mole % of CH_4 in feed 70%)

Stream No.	1	2	3	4	5	6	7	8	9	10	11	12	13
Total flow (kmol/h)	697	512	4,579	4,579	217	209	4,362	4,362	32	4,394	20	452	499
Temperature (°C)	25	39	39	70	40	25	99	80	25	25	25	25	25
Pressure (kPa)	121	120	121	205	200	1,800	200	200	101	120	300	300	1,700
Component (kmol/h)													
CO_2	209	-	282	282	209	209	73	73	-	73	-	-	-
CH_4	488	488	-	-	-	-	-	-	-	-	-	488	488
H_2O	-	24	3,808	3,808	8	-	3,800	3,800	32	3,832	20	4	1
MEA	-	-	488	488	-	-	488	488	-	488	-	-	-

Table A10. Major stream information of CBM separation process (mole % of CH_4 in feed 65%)

Stream No.	1	2	3	4	5	6	7	8	9	10	11	12	13
Total flow (kmol/h)	697	476	5,317	5,317	253	244	5,064	5,064	32	5,096	19	457	453
Temperature (°C)	25	41	40	70	40	25	99	80	25	25	25	25	25
Pressure (kPa)	121	120	121	205	200	1,800	200	200	101	120	300	300	1,700
Component (kmol/h)													
CO_2	244	-	327	327	244	244	84	84	-	84	-	-	-
CH_4	453	453	-	-	-	-	-	-	-	-	-	453	453
H_2O	-	23	4,426	4,426	9	-	4,417	4,417	32	4,449	19	4	0
MEA	-	-	564	564	-	-	564	564	-	564	-	-	-

Table A11. Major stream information of CBM separation process (mole % of CH_4 in feed 60%)

Stream No.	1	2	3	4	5	6	7	8	9	10	11	12	13
Total flow (kmol/h)	697	440	6,062	6,062	289	289	5,773	5,773	32	5,805	19	422	419
Temperature (°C)	25	40	40	70	40	35	99	79	25	25	25	25	25
Pressure (kPa)	121	120	121	205	200	1,800	200	200	101	120	300	300	1,700
Component (kmol/h)													
CO_2	279	-	373	373	279	279	94	94	-	94	-	-	-
CH_4	418	418	-	-	-	-	-	-	-	-	-	418	418
H_2O	-	22	5,051	5,051	10	1	5,041	5,041	32	5,073	19	4	1
MEA	-	-	638	638	-	-	638	638	-	638	-	-	-

Table A12. Major stream information of CBM separation process (mole % of CH_4 in feed 57%)

Stream No.	1	2	3	4	5	6	7	8	9	10	11	12	13
Total flow (kmol/h)	697	418	6,468	6,468	311	300	6,157	6,157	32	6,189	18	400	397
Temperature (°C)	25	43	40	70	40	25	99	80	25	25	25	25	25
Pressure (kPa)	121	120	121	205	200	1,800	200	200	101	120	300	300	1,700
Component (kmol/h)													
CO_2	300	-	401	401	300	300	102	102	-	102	-	-	-
CH_4	397	397	-	-	-	-	-	-	-	-	-	397	397
H_2O	-	21	5,383	5,383	11	-	5,372	5,372	32	5,404	18	3	0
MEA	-	-	684	684	-	-	684	684	-	684	-	-	-

Table A13. Major stream information of CBM separation process (mole % of CH_4 in feed 54%)

Stream No.	1	2	3	4	5	6	7	8	9	10	11	12	13
Total flow (kmol/h)	697	396	6,900	6,900	332	321	6,567	6,567	32	6,599	17	379	376
Temperature (°C)	25	43	40	71	40	25	99	80	25	25	25	25	25
Pressure (kPa)	121	120	121	205	200	1,800	200	200	101	120	300	300	1,700
Component (kmol/h)													
CO_2	321	-	429	429	321	321	108	108	-	108	-	-	-
CH_4	376	376	-	-	-	-	-	-	-	-	-	376	376
H_2O	-	20	5,742	5,742	12	-	5,730	5,730	32	5,762	17	3	0
MEA	-	-	729	729	-	-	729	729	-	729	-	-	-

Table A14. Major stream information of CBM separation process (mole % of CH_4 in feed 50%)

Stream No.	1	2	3	4	5	6	7	8	9	10	11	12	13
Total flow (kmol/h)	697	368	7,467	7,467	361	349	7,106	7,106	21	7,138	16	352	349
Temperature (°C)	25	41	41	71	40	25	99	80	25	25	25	25	25
Pressure (kPa)	121	120	121	205	200	1,800	200	200	101	120	300	300	1,700
Component (kmol/h)													
CO_2	349	-	465	465	348	348	117	117	-	117	-	-	-
CH_4	349	349	-	-	-	-	-	-	-	-	-	349	349
H_2O	-	19	6,223	6,223	13	1	6,210	6,210	32	6,242	16	3	1
MEA	-	-	788	788	-	-	788	788	-	788	-	-	-

Table A15. Major stream information of CBM separation process (mole % of CH_4 in feed 45%)

Stream No.	1	2	3	4	5	6	7	8	9	10	11	12	13
Total flow (kmol/h)	697	331	8,195	8,195	397	383	7,797	7,797	32	7,829	15	316	314
Temperature (°C)	25	44	41	71	40	25	100	80	25	25	25	25	25
Pressure (kPa)	121	120	121	205	200	1,800	200	200	101	120	300	300	1,700
Component (kmol/h)													
CO_2	383	-	512	512	383	383	129	129	-	129	-	-	-
CH_4	314	314	-	-	-	-	-	-	-	-	-	314	314
H_2O	-	18	6,819	6,819	14	-	6,805	6,805	32	6,837	15	2	-
MEA	-	-	864	864	-	-	864	864	-	864	-	-	-

Table A16. Major stream information of CBM separation process (mole % of CH_4 in feed 40%)

Stream No.	1	2	3	4	5	6	7	8	9	10	11	12	13
Total flow (kmol/h)	697	295	8,865	8,865	434	420	8,442	8,442	32	8,464	14	281	279
Temperature (°C)	25	41	42	71	40	25	100	81	25	25	25	25	25
Pressure (kPa)	121	120	121	205	200	1,800	200	200	101	120	300	300	1,700
Component (kmol/h)													
CO_2	418	-	557	557	418	418	138	138	-	138	-	-	-
CH_4	279	279	-	-	-	-	-	-	-	-	-	279	279
H_2O	-	16	7,374	7,374	15	1	7,358	7,358	32	7,390	14	2	-
MEA	-	-	935	935	-	-	935	935	-	935	-	-	-

Table A17. Major stream information of CBM separation process (mole % of CH_4 in feed 35%)

Stream No.	1	2	3	4	5	6	7	8	9	10	11	12	13
Total flow (kmol/h)	697	259	9,672	9,672	470	455	9,202	9,202	33	9,235	14	246	244
Temperature (°C)	25	42	42	74	40	25	101	84	25	25	25	25	25
Pressure (kPa)	121	120	121	205	200	1,800	200	200	101	120	300	300	1,700
Component (kmol/h)													
CO_2	453	-	606	606	453	453	153	153	-	153	-	-	-
CH_4	244	244	-	-	-	-	-	-	-	-	-	244	244
H_2O	-	15	8,047	8,047	17	1	8,030	8,030	33	8,063	14	2	-
MEA	-	-	1,020	1,020	-	-	1,020	1,020	-	1,020	-	-	-

Table A18. Energy consumption and energy efficiency of the CBM separation systems over time in HSC case

Facility operation time (year)	1	2	3	4	5	6	7	8	9	10	11	12
CH_4 content in CBM feed gas (%)	90	88	86	84	82	80	77	74	70	65	60	50
(a) Heat flux of feed (MW)	154.7	151.3	147.9	144.4	141.0	137.5	132.4	127.2	120.3	111.8	103.2	86.0
(b) Total consumed energy (MW)	3.5	4.0	4.5	5.1	5.6	6.2	7.0	7.8	9.0	10.2	10.2	14.0
Electricity consumption (MW)	1.1	1.1	1.1	1.1	1.1	1.1	1.1	1.1	1.1	1.0	1.0	1.0
Steam consumption (MW)	2.4	2.9	3.5	4.0	4.6	5.1	5.9	6.7	7.9	9.2	10.6	12.9
(c) Heat flux of product (MW)	154.7	151.3	147.9	144.4	141.0	137.5	132.4	127.2	120.3	111.8	103.2	86.0
Process energy efficiency (=(c)/(a)+(b)) (%)	**97.5**	**97.1**	**96.7**	**96.2**	**95.8**	**95.3**	**94.5**	**93.6**	**92.4**	**90.8**	**88.9**	**84.7**

Table A19. Energy consumption and energy efficiency of the CBM separation systems over time in LSC case

Facility operation time (year)	1	2	3	4	5	6	7	8	9	10	11	12
CH_4 content in CBM feed gas (%)	90	80	77	74	70	60	57	54	50	45	40	35
(a) Heat flux of feed (MW)	154.7	137.5	132.4	127.2	120.3	103.2	98.0	92.8	86.0	77.4	68.8	60.2
(b) Total consumed energy (MW)	3.5	6.2	7.0	7.8	9.0	11.6	12.4	13.2	14.0	15.7	17.0	18.6
Electricity consumption (MW)	1.1	1.1	1.1	1.1	1.1	1.0	1.0	1.0	1.0	1.0	1.0	1.0
Steam consumption (MW)	2.4	5.1	5.9	6.7	7.9	10.6	11.4	12.2	12.9	14.7	16.0	17.6
(c) Heat flux of product (MW)	154.7	137.5	132.4	127.2	120.3	103.2	98.0	92.8	86.0	77.4	68.8	60.2
Process energy efficiency (=(c)/(a)+(b)) (%)	**97.5**	**95.3**	**94.5**	**93.6**	**92.4**	**88.9**	**87.7**	**86.3**	**84.7**	**81.6**	**78.4**	**74.4**

Table A20. A breakdown of the total capital investment cost of amine absorption plant

Cost allocation	Cost ($)
Direct cost	11,891,174
Purchased equipment	4,423,800
Equipment installation	2,335,766
Instrumentation and control	884,760
Piping	1,769,520
Electrical installation	486,618
Building and building services	442,380
Yard improvements	442,380
Services facilities	884,760
Land	221,190
Indirect cost	4,459,190
Engineering	1,189,117
Construction expenses	1,189,117
Contractor's fee	59,279
Contingency	2,021,677
Fixed capital investment cost (FCI) =Direct cost+Indirect cost	16,350,365
Working capital	4,087,591
Total capital investment cost (TCI) =Fixed capital investment cost+Working capital	20,437,956